

## **LES of the Ignition Process of Non-premixed CH<sub>4</sub> based on Dynamic Thickened Flame Model**

Jiang Yang<sup>a</sup>, Lei Yubing<sup>b</sup>, Gao Apeng<sup>c</sup>

Nanjing University of Aeronautics and Astronautics, Jiangsu Province's Key Laboratory  
of Aerospace Power System, Nan Jing 210016

<sup>a</sup>1183034087@qq.com, <sup>b</sup>leiyb@nuaa.edu.cn, <sup>c</sup>285641583@qq.com

**Keywords:** ignition, large Eddy simulation, dynamic thickening flame model, Gauss heat source.

**Abstract.** Improve the accuracy of ignition calculate simulation through dynamic thickening of the of flame front in order to achieve Large Eddy Simulation (LES) solution scales. Taking the WALL model which takes the sticky near the wall into account as the sub-grid turbulence model, simulating the process of energy releasing of spark plug by the way of adding Gauss heat source to the energy function. 40ms of the ignition process is calculated based on the cold state flow field, and compare the numerical simulation results with corresponding experimental results abroad. It shows: The simulation accuracy of cold flow field of LES is good, and be able to capture small-size vortex; Large Eddy Simulation based on dynamic thickening flame model is an effective method to predict the dynamic diffusion processes of CH<sub>4</sub> non-premixed flame; Recirculation zone plays an important role of fuel distribution, flame spread and stability.

### **1. Introduction**

Ignition is a non-steady state processes with different kinds of combustion forms at different locations and time. There may be pre-mixed, non-premixed or partially-premixed combustion forms. Boileauet and the others <sup>[1]</sup> carried out a simulation on forced ignition of a premixed reflux combustion chamber with Artificial Thickened Flame (ATF) model proposed by Colin<sup>[2]</sup>. The dynamic diffusion process of the flame in the whole ring is analyzed, it is found that the atomization effect of the nozzle has an important influence on the ignition performance of the combustion chamber. Lacaze<sup>[3]</sup> studied the ignition process of CH<sub>4</sub> turbulent premixed combustion with LES method based on the thickening flame model based on the experiment results of Ahmed<sup>[4]</sup>. The dynamic thickened flame model was optimized by Legier<sup>[5]</sup> based on the ATF model and taken both premixed and non-premixed flame situation into account, and Dynamic Thickening Flame (DTF) model was proposed at last. And a two-dimensional test example is given, the simulation results are in good agreement with the DNS. Truffin<sup>[6]</sup> applied the dynamic thickening flame model to three-dimensional partial premixed combustion. And prediction result is quite good. However, the study of dynamic thickening flame model for non-premixed turbulent combustion ignition is rarely reported for the time being.

### **2. Numerical simulation method**

#### **2.1 Calculation model and mesh**

In this paper, the CH<sub>4</sub> / Air burner of S.F.Afmed et al<sup>[7]</sup> of Cambridge University was used as the model as shown in Fig.1. The model consists of two coaxial cylindrical channels, air channel diameter  $D_a = 35\text{mm}$ , fuel passage diameter  $D_c = 7\text{ mm}$ , fuel channel park conical blunt body end diameter  $D_n = 25\text{mm}$  and with 45 degrees vertebral angle, blocking ratio is 50%, CH<sub>4</sub> jet groove locate at 2mm from the vertebral, the width is 0.7 mm. The central reflow burner length  $L = 200\text{ mm}$ , Diameter  $D = 70\text{ mm}$ .

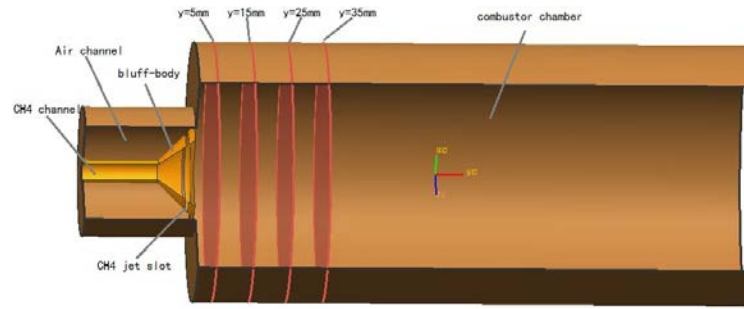


Fig.1 Geometric model

Fig.2 is the grid of this paper, mainly using O-structured grid, near the wall at the mesh encryption, the wall  $Y^+$  is less than 1, the grid volume 3576701, the number of nodes 3526240.

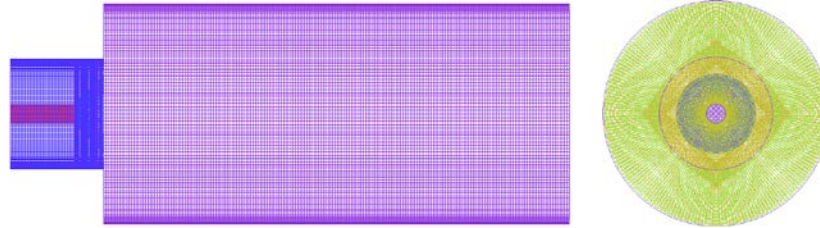


Fig.2 Computational grid

## 2.2 Dynamic thickening flame model

### 2.2.1 Basic theory

The flame front is a region where the chemical reaction and turbulence interaction are relatively intense, and the gradient of flow and combustion reaction parameters is large in this region. And the thickness of the flame front is very small, for the millimeter level, if the grid scale is not small enough, it is difficult to simulate accurately, and it will greatly increase the calculation time while increase the number of the grids. According to the Dynamic Thickening Flame model proposed by O.Colin<sup>[2]</sup> et al, the laminar flame propagation velocity ( $s_l^0$ ) is proportional to the root ( $\sqrt{D\omega}$ ) of product of the diffusion coefficient (D) and the chemical reaction rate ( $\omega$ ); The laminar flame thickness ( $\delta_l^0$ ) is proportional to the quotient ( $D/s_l^0$ ) of diffusion coefficient (D) and the laminar flame propagation velocity ( $s_l^0$ ). The diffusion coefficient of each reaction component is increased ( $F \times D$ ) by the thickening coefficient F while the chemical reaction Arrhenius constant A ( $A/F$ ) is decreased. The propagation velocity of the laminar premixed flame will remain unchanged, but the flame thickness will increase ( $F \times \delta_l^0$ ); adjust the thickening coefficient F to the appropriate value, it can increase the flame front thickness, making the flame front contains enough grid nodes, can be much more accurate to capture the process of dynamic diffusion of flame. And a detection function similar to the Arrhenius chemical reaction rate is introduced, so that the model is effective only in the reaction zone while the thickening coefficient is kept equal to 1 outside the reaction zone. The obvious advantage of this method is that the flame surface is thickened only at the flame front, and the diffusion coefficient is not modified outside the flame surface area. As the flame surface is artificially thickened, the small-scale turbulence pulsation on the flame surface wrinkle is weakened, Angelberge<sup>[8]</sup> and Colin<sup>[2]</sup> proposed the efficiency function E to simulate the small-scale turbulence pulsation on the flame surface folds effect.

### 2.2.2 Dynamic thickening factor

In order to distinguish the different combustion areas in the calculation, a function similar to Arrhenius chemical reaction rate expression is used as the detection function:

$$\Omega = Y_F^{V_f} Y_O^{V_o} \exp\left(-\Gamma \frac{E_a}{RT}\right) \quad (1)$$

$Y_F$  is the fuel mass fraction,  $Y_O$  is the oxidant mass fraction,  $V_f$  and  $V_o$  are the exponential factors of the fuel and the oxidant, respectively 0.5 and 1.0.  $E_a$  is the reaction activation energy.

Thickening coefficient expression is as follows:

$$F = 1 + (F_{\max} - 1) \tanh\left(C_F \frac{\Omega}{\Omega_0}\right) \quad (2)$$

$F_{\max}$  is the maximum value of the thickening coefficient in the calculation domain, taking 10 in this paper. That means, there are about ten grid nodes in the flame front to capture the flame propagation characteristics;  $\Omega_0$  is the maximum value of the detection function in the calculation. In this paper, we first calculate the value of  $\Omega_0$  by using the premix reactor in Chemkin, and it is  $1 \times 10^{-9}$ .  $C_F$  is the coefficient to control the transition between the thickened and non-thickened regions, takes  $C_F = 0.5$  in this paper.

### 2.2.3 Efficiency function

The above dynamic thickening flame model maintains the flame propagation speed, but the effect of small-scale turbulence is weakened because of the increase of flame surface thickness. In order to solve this problem, Angelberge<sup>[8]</sup> and Colin<sup>[2]</sup> proposed using the efficiency function  $E$  to consider the small-scale turbulence on the flame surface wrinkle:

$$E = \frac{E(\delta_l^0)}{E(\delta_l)} = \frac{1 + \alpha \Gamma_{\Delta_e} \left( \frac{\Delta_e}{\delta_l^0}, \frac{u'_{\Delta_e}}{s_l^0} \right) \frac{u'_{\Delta_e}}{s_l^0}}{1 + \alpha \Gamma_{\Delta_e} \left( \frac{\Delta_e}{\delta_l}, \frac{u'_{\Delta_e}}{s_l} \right) \frac{u'_{\Delta_e}}{s_l}} \quad (3)$$

$\delta_l$  is the thickness of the thickening of the flame;  $\alpha$  is the model coefficient, which can be deduced from the theory of Damoukel;  $\Delta_e$  is the filter scale,  $u'_{\Delta_e}$  is the sub-grid turbulence; expression of  $\Gamma_{\Delta_e}$  function is :

$$\Gamma_{\Delta_e} \left( \frac{\Delta_e}{\delta_l}, \frac{u'_{\Delta_e}}{s_l} \right) = 0.75 \exp \left[ -\frac{1.2}{(u'_{\Delta_e} / s_l)^{0.3}} \right] \left( \frac{\Delta_e}{\delta_l} \right)^{2/3} \quad (4)$$

$\delta_l^0$  is the laminar flame thickness,  $s_l^0$  is the laminar flame propagation velocity, the calculation is as follows:

For the central reflux burner model used in this paper, the turbulence intensity is larger in the recirculation zone, CH<sub>4</sub> and air mixture are more sufficient, which can be regarded as premixed combustion. According to the experimental data of the flame propagation velocity of different equivalence ratios of Andrews et al<sup>[9]</sup>, the cubic function expression of the CH<sub>4</sub> laminar flame propagation velocity with respect to the equivalence ratio is obtained as shown in Fig.4

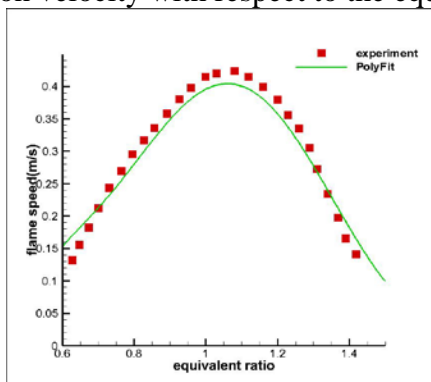


Fig.3 Laminar flame propagation velocity

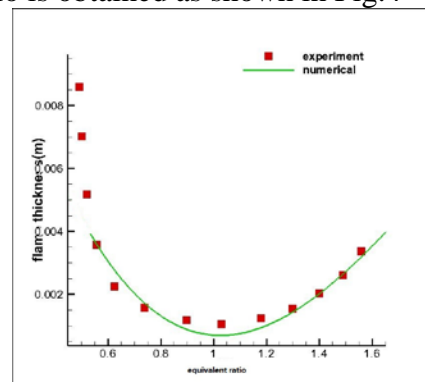


Fig.4 Laminar flame thickness

$$Y = A + BX + CX^2 + DX^3 \quad (5)$$

Where:  $A = -0.05387$ ,  $B = 0.06199$ ,  $C = 1.36753$ ,  $D = -1.040125$ .

Laminar flame thickness is solved by the Blint laminar flame thickness correction approximate equation which used to large eddy simulation:

$$\delta_L^0 = \delta \cdot C_B \left( \frac{T^b}{T^u} \right)^\beta \quad (6)$$

$\delta$  is the thermal diffusion rate which can be obtained through the UDF;  $C_B$  is the thickness coefficient, the default is 2.0;  $\beta$  is the temperature index, the default is 0.7;  $T_b$  is the adiabatic gas temperature, adiabatic temperature of  $CH_4$  is 2000K;  $T_u$  is the temperature of the unburned gas, the temperature of intake air is 300K. The results of flame thickness calculation are shown in Fig. 4, which agrees well with the experimental results.

### 2.3 Ignition model of spark plug

In this paper, use the way of adding source term to the energy equation<sup>[5]</sup> to simulate the spark ignition. The spark plug model is shown in Equation 7.

$$\omega_{spark} = \frac{E_{spark}}{(2\pi)^2 \sigma_i \sigma_r^3} e^{-\frac{1}{2} \left[ \left( \frac{t-t_0}{\sigma_i} \right)^2 + \left( \frac{x-x_0}{\sigma_r} \right)^2 + \left( \frac{y-y_0}{\sigma_r} \right)^2 + \left( \frac{z-z_0}{\sigma_r} \right)^2 \right]} \quad (7)$$

$\omega_{spark}$  is the spark plug model heat release rate, in unit of KJ-mm-3-s-1;  $E_{spark}$  is the ignition energy, in units of J;  $\sigma_i$  is the ignition delay time, the typical spark plug ignition delay time is 0.16ms;  $\sigma_r$  is the flame core radius, is 2mm reference to the experimental data.  $(x_0, y_0, z_0)$  is the ignition location;  $t$  is the calculation time of duration,  $t_0$  is the start time of the ignition.

### 2.4 Boundary conditions

Inlet velocity of air is 10m/s, inlet velocity of  $CH_4$  is 5m/s, inlet temperature is 300K, mass fraction of  $CH_4$  is 0.055; working pressure of combustion chamber is atmospheric pressure, time step is solved by CFL criterion:

$$C_{FL} = \frac{\Delta t (|u|_{max} + c)}{\Delta x} < 1 \quad (8)$$

$$\Delta t = \frac{\Delta x}{(|u|_{max} + c)} C_{FL} \quad (9)$$

$c$  is the local speed of sound;  $u_{max}$  is the max velocity in the flow field;  $\Delta x$  is the minimum grid size. In this paper,  $CFL = 0.6$ ,  $\Delta x = 1mm$ ,  $c = 340m/s$ , the maximum velocity  $u_{max}$  in the flow field is 12m/s according to the experimental data. So in this paper, the time-step is  $\Delta t = 2 \times 10^{-6}$ , calculated the dynamic diffusion process of ignition for 40ms,  $2 \times 10^4$  time steps. Ignition position is (0,0,25) according to the experiment, ignition energy is 0.2J, ignition duration time is 0.5ms.

## 3. Numerical simulation results and analysis

### 3.1 The flow of non-ignition

The result of cold flow is shown in Fig.5, the period of flow is 10ms based on the monitor parameters. (a), (b), (c) are the time-averaged results within 10ms of LES; (a'), (b'), (c') are the transient results of LES. The length of the reflux zone is 25mm as shown in Fig.5b, which is in good agreement with the experimental value.

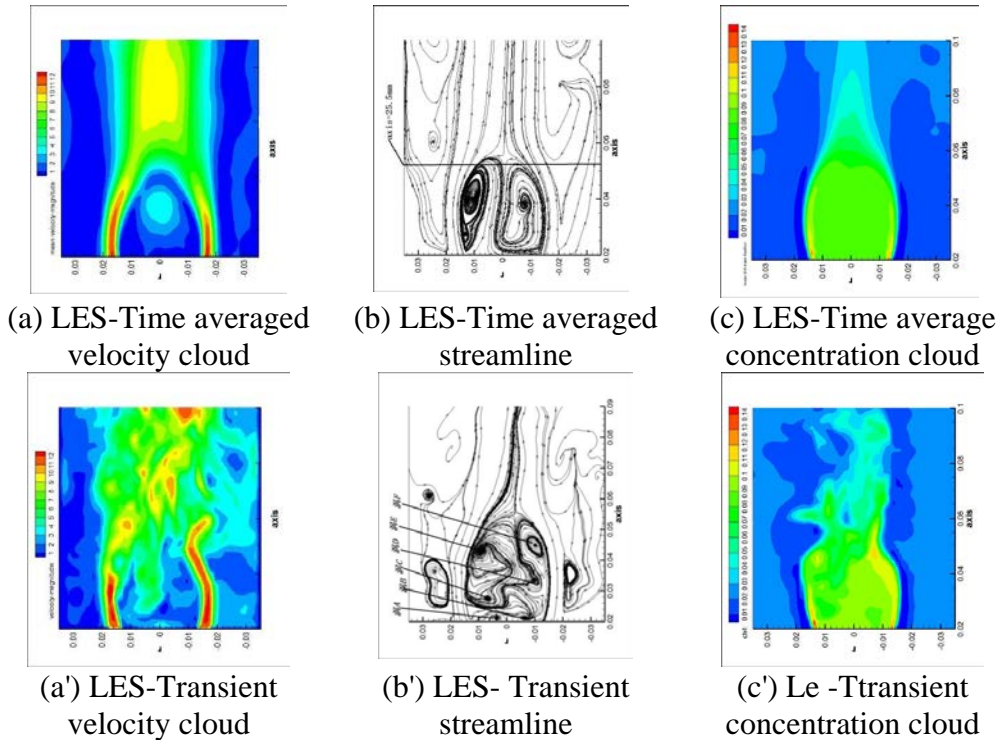


Fig.5 Cold flow field cloud of LES

The velocity and concentration results of the numerical simulation of the axial sections in the recirculation zone and the downstream area of the recirculation zone are compared with the experimental results in order to verify the accuracy of calculation of the cold flow. Within the five sections,  $Y = 0.22D_n$ ,  $y = 0.62D_n$ ,  $y = 1.0D_n$ ,  $y = 1.4D_n$ ,  $y = 2.0D_n$ . The axial velocity and concentration agree well with the experimental results, as shown in Fig.6. In this figure, the value of the coordinate is dimensionless, the X coordinate of Fig.6a, b is divided by the tapered blunt body diameter  $D_n$ , the Y ordinate of Fig.6a is divided by the inlet air velocity  $V_b$ .

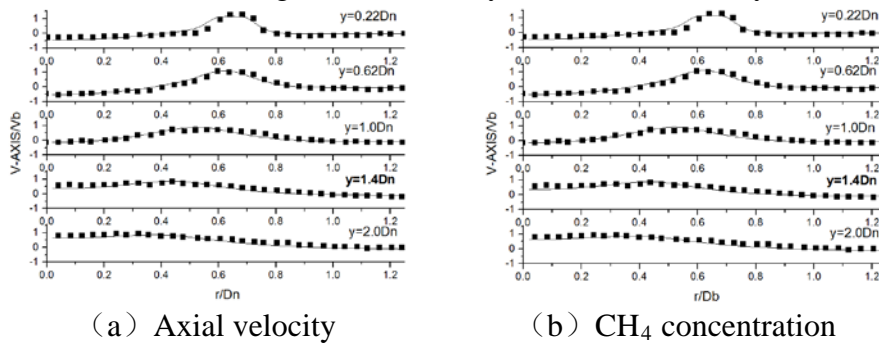


Fig.6 Comparison of unburned and experimental data ■: experiment —: LES  
 $D_n=25\text{mm}$   $V_b=10\text{m/s}$

### 3.2 Analysis of the ignition process

At the working stage of the igniter, the relationship between the heat source and the maximum temperature with time is shown in Fig.7. At the initial stage, the energy is mainly released by the Gauss heat source, the maximum temperature grows smoothly. The heat released by the reaction and the maximum temperature increase suddenly when the temperature reaches the effective value to trigger CH<sub>4</sub>-Air chemical reaction. At the time of 0.15ms, heat released by the Gauss heat source began to reduce, the maximum temperature maintained at the range of CH<sub>4</sub> combustion temperature, ignition is success.

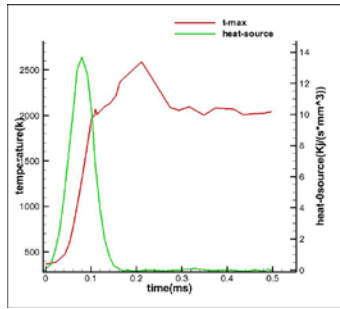


Fig.7 Reaction parameter-time

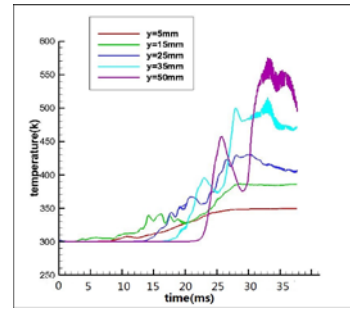


Fig.8 Temperature of the axial section-time

The average temperature-time curves of different axis sections are shown in Fig.8. The temperature increases slowly at 0-10ms, mainly because the flame core is in the initial state, has not yet begun a large-scale diffusion; From 10ms to 20ms, temperature of reflux zone rises faster as shown in Fig. 9a, mainly because the ignition position is located at the downstream boundary of the recirculation zone, the flame begins to flow into the recirculation zone under the action of the backflow, and the flame surface begins to fold under the action of turbulence. After 20ms, the average temperature of the downstream section began to rise as shown in Fig.9b, the flame is nearly full of the entire reflux zone, the flame began to spread downstream under the action of jet flow. At the same time, the flame developed into W-like under the action of large vortex E' and vortex F' downstream.

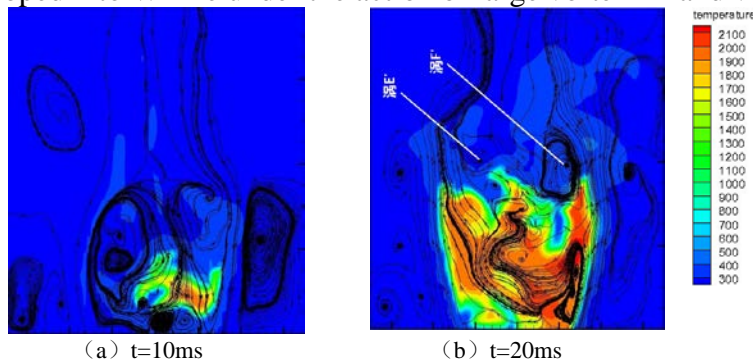
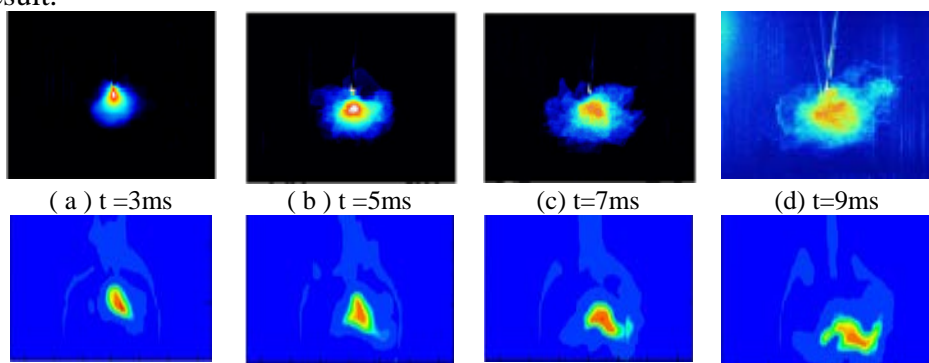


Fig.9 Temperature and streamline at different time(Image size70×80mm)

The two-dimensional view of the flame spread within 30ms of the ignition process at the center cross section of the over-ignition position is shown in Fig.10. (a') ~ (n') are the numerical simulation results based on the dynamic thickened flame model, (a) ~ (n) are the corresponding experimental result<sup>[10]</sup>. It can be seen from the numerical simulation results that the flame core triggered by the heat source is almost formed and become ellipsoidal shape at 3ms, and begin to heat the unburned mixed gases near the core; 3ms to 9ms, the flame propagates into the reflux zone under the action of the return flow, the turbulence intensity in the recirculation zone is larger and the flame peak begin to spread gradually. And the flame propagates into a conical type which is consistent with the cosine law of flame propagation; At 15ms the flame spreads to the shear layer and propagates downstream along the boundary of the recirculation zone; After 30ms, the flame substantially fills the entire combustion zone and become stable. It can be seen that the result of numerical simulation agrees well with the experiment result.



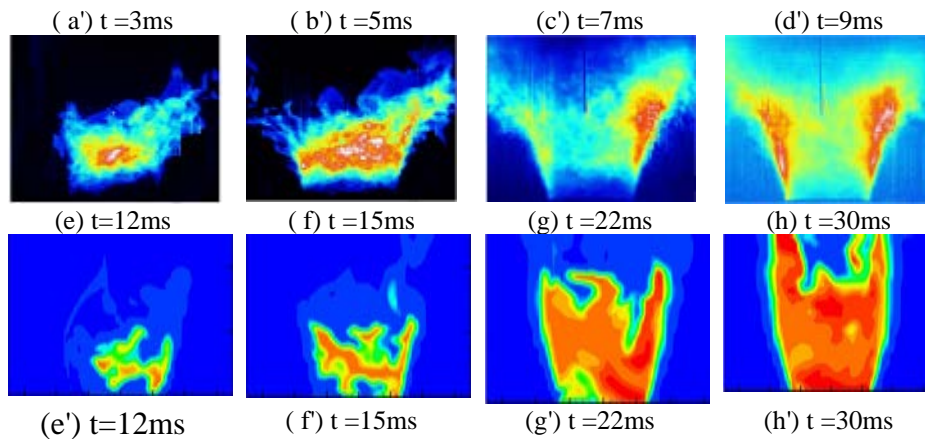


Fig.10 The dynamic evolution of the flame during ignition (Image size  $70 \times 50\text{mm}$ )

The movement of the flame front can be analyzed by a sudden change of reaction rate as shown in Fig.11. At the initial stage of ignition, the flames first diffuse into the reflux zone under the action of reflux,  $\text{CH}_4$  reaction rate of  $y=15\text{mm}$ ,  $5\text{mm}$  sections accelerates suddenly at  $10\text{ms}$ , indicating that the flame surface has diffused into the interior of the reflux zone; The reaction rate of  $y=35\text{mm}$  section also increased gradually at  $16\text{ms}$ , indicating that the flame surface has begun to spread to the downstream area;

The reaction rate of  $y = 50\text{mm}$  section begins to increase at  $25\text{ms}$ , the flame surface has spread to twice the length of the reflux zone, and the reaction rate of  $y = 15\text{mm}$ ,  $5\text{mm}$  sections begin to rise and gradually stabilize, indicating that the flame has basically filled the entire upstream area, the flame began to stabilize. Fig.12 shows the corresponding concentration-time curve.

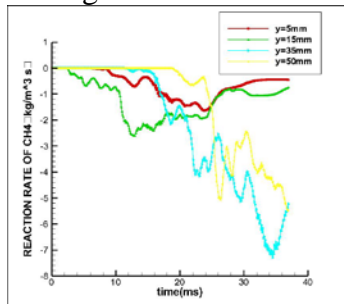


Fig.11 Average reaction rate of  $\text{CH}_4$  at axial position

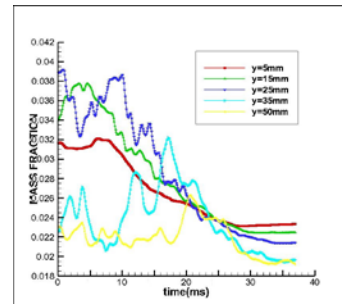


Fig.12 Average concentration of  $\text{CH}_4$  at axial position

#### 4. Conclusions

Large Eddy Simulation of non-premixed  $\text{CH}_4$  ignition process based on Dynamic Thickened Flame Model was carried out in this paper, studied on the cold flow of non-ignition and flame dynamic diffusion of the ignition process. Draw the following conclusions:

(1): Before the ignition, LES of cold state results are in good agreement with the experimental results, speed, concentration of  $\text{CH}_4$  of different axial cross sections are in good agreement with experimental values. LES method could capture smaller structure vortex which can be used to simulate the effect of turbulence on flame.

(2): In the  $30\text{ms}$  calculation process, the dynamic thickening flame model can simulate the flame dynamic diffusion process well in the ignition time and flame size position and experimental results consistent. Large Eddy Simulation based on dynamic thickening flame model is an effective method to predict the dynamic diffusion processes of  $\text{CH}_4$  non-premixed flame.

## 5. References

- [1] M. Boileau, G. Sta\_elbach, B. Cuenot, and T. Poinso. LES of an ignition sequence in a gas turbine engine. *Combustion and Flame*, 154:2\_22, 2008.
- [2] O. Colin, F. Ducros, D.Veynante, and T. Poinso. A thickened flame model for large eddy simulations of turbulent premixed combustion. *Physics of fluids*, 12(7):1843\_1863, 2000.
- [3] G.Lacaze, E. Richardson, and T.Poinso. Large eddy simulation of spark ignition in a turbulent methane jet. *Combustion and Flame*, 156(10):1993 \_ 2009, 2009.
- [4] S. F. Ahmed, R.Balachandran, T. Marchione, and E.Mastorakos. Spark ignition of turbulent non-premixed bluff body flames. *Combustion and Flame*, 151:366\_385,2007.
- [5] Legier JP ,Poinso T.Veynante. Dynamically thickened flame LES model for premixed and non-premixed turbulent combustion[C]// *Proceedings of the Summer Program 2000*. Stanford, 2000: 157-168.
- [6] Truffin P K. Simulation aux grandes échelles et identification acoustique des turbines à gaz enrégime partiellement prémélangé[D]. Toulouse: INP Toulouse, 2005.
- [7] Jones W P, Tyliczszak A. Large eddy simulation of spark ignition in a gas turbine combustor[J]. *Flow, turbulence and combustion*, 2010, 85(3-4): 711-734.
- [8] Angelberger C Veynante D, Egolfopoulos F, et al. Large eddy simulation of combustion instabilities in turbulent premixed flames[C]// *Proceedings of the Summer Program 1998*. Stanford, 1998: 61-82.
- [9] Andrews, G.E., and Bradley, D., “The Burning Velocity of Methane-Air Mixtures,” *Combustion and Flame*, 19:275-288(1972).
- [10] S.F. Ahmed a, R. Balachandranb, T. Marchione a, E. Mastorakos a. Spark ignition of turbulent non-premixed bluff-body flames. *Combustion and Flame* 151 (2007) 366–385.